Environmental Science and Pollution Research
May 2017, Volume 24, Issue 15, Pages 13797-13807
http://dx.doi.org/10.1007/s11356-017-8972-y
http://archimer.ifremer.fr/doc/00382/49330/

In situ measurement with diffusive gradients in thin films: effect of biofouling in freshwater

Uher Emmanuelle [1, 2, *], Compère Chantal [3], Combe Matthieu [1], Mazeas Florence [3], Gourlay-Francé Catherine [1, 2, 4]

[1] Irstea, UR HBAN Hydrosystèmes et BioprocédésAntony Cedex,France
[2] FIRE FR-3020Paris,France
[3] IFREMER, Centre de Bretagne, ZI de la Pointe du DiablePlouzané,France
[4] AnsesMaisons-Alfort Cedex,France

* Corresponding author : Emmanuelle Uher, email address : emmanuelle.uher@irstea.fr

Abstract :

Concerning in situ passive sampler deployment, several technical priorities must be considered. In particular, deployment time must be sufficiently long not only to allow a significant quantity to be accumulated to facilitate analysis but also to ensure that the signal is above the quantification limit and out of the blank influence. Moreover, regarding the diffusive gradient in thin films (DGT) technique, deployment time must also be sufficiently long (at least 5 days) to avoid the interactions of the solutes with the material diffusion layer of the DGT and for the steady state to be reached in the gel. However, biofouling occurs in situ and modifies the surface of the samplers. In this article, we propose a kinetic model which highlights the biofouling effect. This model was able to describe the mitigation of the flux towards the DGT resin observed on Cd, Co, Mn, Ni and Zn during a 22-day deployment in the Seine River. Over a period of 22 days, biofouling had a significant impact on the DGT concentrations measured, which were decreased twofold to threefold when compared to concentrations measured in unaffected DGTs.

Keywords : DGT, Metals, Biofouling, Seine River, Field deployment, Passive sampler

1. Introduction

Passive samplers are an emerging way of assessing water quality. Their use is increasing in the scientific community. It is claimed that they provide time-integrated concentrations of the species they measure during their deployment in water. Quantification limits are lowered and the matrix effects in the analytical process are reduced. However, *in situ* conditions differ significantly from convenient laboratory conditions. Biofouling occurs at the surface of the samplers being immersed in water. In freshwater, physicochemical conditions differ greatly between sampling sites, while deployment time is subjected to many constraints: metal accumulation must be significant, whereas, in relatively uncontaminated sites, this may require a long deployment time, and interactions of the solutes with the material diffusion layer cannot be neglected if the deployment time is too short. Diffusion of metals may be retarded at the beginning of the deployment because of these interactions, and deployment time has to be sufficiently long to ensure the steady state is reached, as is discussed by Davison and Zhang (2012) and Garmo *et al.* (2008b,a).

Previous studies examined what consequences the presence of major ions had on diffusive gradient in thin film (DGT) measurements in marine water (Tankere-Muller *et al.* 2012). They also simulated the limits of the linear accumulation regime of DGT concerning pH, deployment time, and dissolved ligands (Mongin *et al.* 2013). Others studies showed that biofouling might affect DGT measurement: Pichette *et al.* (2007) and Feng *et al.* (2016) studied the effect of biofilm development on phosphate measurement using DGT, respectively in a freshwater aquaculture pond and in freshwater. It has already been observed that biofouling had a strong effect on DGT measurement in raw wastewater (Uher *et al.* 2012). However, Buzier *et al.* showed that 14-day-biofouling did not affect the diffusion coefficient of the DGT diffusion layer in freshwater (Buzier *et al.* 2014).

Biofilm developing at the surface of DGT has long been suspected to behave as an additional inert diffusion layer, which may reduce the uptake of the species analyzed (Booij *et al.* 2006, Pichette *et al.* 2007, Schafer *et al.* 2008). Moreover, it has long been known that biofilm interacts with metals in solution through various processes (Van Hullebusch *et al.* 2003). One of these processes, biosorption on biofilms and bacterial cells has been studied in depth as a potential sorbing material for removing metals from waste solutions (Ginisty *et al.* 1998, Kuyucak and Volesky 1988, Veglio and Beolchini 1997, Wase and Wase 2002). Other interactions of varying importance and reversibility

may occur between biofilm and metals, namely: complexation, precipitation of insoluble salts, adsorption on iron and manganese oxides, and reduction, as highlighted both in a comprehensive review by Van Hullebusch *et al*. (2003) of knowledge of the mechanisms of metal immobilization by biofilm and also in several experimental studies conducted under varying conditions and with several metals (Bradac *et al.* 2009a, Bradac *et al.* 2010, Duong *et al.* 2010, Faburé *et al.* 2015, Fechner *et al.* 2014, Moppert *et al.* 2009, Toner *et al.* 2005, White and Gadd 2000). It is also assumed that biofilm is a "gateway" between dissolved metals in solution and hydrous metal oxides coating the streambed, and that biofilm plays a role in the diel cycles of dissolved metals (Nimick *et al*. 2011). More recent reviews have focused on the role of extracellular polymeric substances (EPSs, secreted by microorganisms), which exhibit abundant binding sites for metals (Li and Yu 2014, More *et al*. 2014). Feng *et al*. showed that the composition of a biofilm grown at the surface of DGT phosphate-samplers mainly consisting of diatoms, several metal oxides (Fe, Al, Mn) and EPSs (Feng *et al*. 2016). Buzier *et al*.(2014) also observed biofilm forming at the surface of DGT samplers: biofilm was composed of organic deposits and metallic oxides capable of adsorbing species.

The results of our previous study suggest that biofilms at the surface of DGTs and metal species interact (Uher *et al*. 2012). Different effects were observed depending on the metal being studied (Cd, Cr, Co, Cu, Mn, Ni, Pb, Zn). It was concluded from these results that biofilm exhibits metal-binding properties with varying degrees of specificity and affinity, depending on the metal under scrunity. Furthermore, the literature suggests that metal-binding properties also depend on the bulk solution chemistry and on the physiological state of the biofilm (Nimick *et al.* 2011). The biofilm's composition is likely to vary according to the sampling site and deployment conditions. Thus, biofouling can also be expected to vary with the sampling site. A simple kinetic model which highlights the physicochemical interactions between metals and biofilms was proposed to explain biofilm's effect on DGT measurement. However, we need to precisely verify whether the description we proposed is valid in other conditions than in wastewater where the former experiments were conducted. DGTs are more often deployed in freshwater. Therefore more freshwater data are needed to establish a model of the impact of biofouling on DGT measurement.

The first purpose of this particular research was to precisely describe how biofouling may affect the transfer of metals to the DGT chelating resin by proposing a quantitative model involving physicochemical interactions of metals and biofilm. Its second purpose was to verify whether this hypothesis is valid in freshwater. A study was

conducted in the Seine River. Accumulation of metals in the DGT Chelex resin was monitored along with biofouling and biomass growth estimation of the biofilm attached to the protective membrane of the DGT, in order to compare the model with the experimental data. Physicochemical conditions and deployment time were considered while discussing the results.

2. Theoretical background

2.1 DGT principle

The principle of DGT is based on Fick's first law. DGTs are composed of a chelating resin, a diffusive hydrogel, and a protective membrane. A metal diffusion gradient develops between the bulk solution and the resin layer because this latter strongly sequesters cationic metals. Consequently, metal species are transported through the material diffusion layer (MDL), comprising of the gel and the membrane, toward the resin. The flux (J) of metal ions can be expressed by Equation 1:

$$J = D_{MDL}\frac{\Delta C}{\Delta_{MDL}} \qquad \text{Equation 1}$$

where D_{MDL} is the diffusion coefficient in the material diffusion layer, ΔC is the concentration gradient, and Δ_{MDL} is the thickness of the MDL. The free metal ions in the diffusion layer are in rapid equilibrium with the resin, so the concentration near the resin is zero. $\Delta C \approx C$, where C is the concentration in the bulk solution. Therefore at steady state Equation 1 becomes:

$$J = D_{MDL}\frac{C}{\Delta_{MDL}} \qquad \text{Equation 2}$$

The flux of species through an area (A) after a given time (t) is also defined by:

$$J = \frac{m}{tA} \qquad \text{Equation 3}$$

where m is the mass of metal accumulated in the chelating resin. It should be noted that J is the mean flux of the metals during the deployment time.

Combining Equation 2 and Equation 3 shown above, the equation giving the concentration in water measured by DGT is as follows:

$$C_{DGT} = \frac{m\Delta_{MDL}}{D_{MDL}tA} \qquad \text{Equation 4}$$

94

95 **2.2 Metal biofilm DGT interaction model**

96 As soon as a substrate is immersed in water, planktonic cells would attach and, through growth and EPS production,
97 biofilms may develop. This biofilm layer both constitutes an additional diffusion layer for DGT and exhibits
98 abundant interaction sites for metals. However, DGT cannot be considered as just any surface in water because of
99 the affinity of metal for chelating resin thereby creating the diffusion gradient in the gel of the DGT device. Thus
100 metals fate may be driven by two different sinks: the diffusion through the DGT gel because of the resin and the
101 binding within the external biofilm. This is illustrated in Figure 1: whenever metals interact with or within the
102 biofilm matrix, they are temporarily fixed by the biofilm. Metals reversibly retained by the biofilm eventually
103 diffuse through the hydrogel toward the resin. If the dissociation of the metal from the biofilm is the limiting step,
104 metal diffusion in the hydrogel might be severely retarded. If the complexes dissociate readily, accumulation of
105 metal in the resin might occur with no significant effect.

106 Two parameters are decisive: firstly the nature of the biofilm which in turn may alter the nature of the interactions
107 with the metals and secondly the metal concentration in water which influences the diffusion gradient force.

108 From Equation 2 and Equation 3 above, we can expect that the flux of metal in DGT is constant if the concentration
109 in water is constant. When a part of the metal is retained by the biofilm, the mean flux J should be reduced to
110 account for that part that does not diffuse because of interactions:

$$J = J_0 - D_{MDL}\frac{\overline{C_B}}{\Delta_{MDL}} \qquad \text{Equation 5}$$

111 where J_0 is the flux in the absence of biofilm and $\overline{C_B}$ is the mean metal concentration immobilized in the biofilm
112 during the deployment time in ng cm^{-3}.
113 Given the reactions shown in Figure 1, the kinetics of metal in the biofilm can be described by Equation 6:

$$\frac{dC_B}{dt} = k_1 C_M - k_2 C_B \qquad \text{Equation 6}$$

114 where C_B is the concentration of metal immobilized in the biofilm and C_M is the concentration of metal M
115 interacting with biofilm in water in the vicinity of the sampler. Considering $C_B = 0$ at time t = 0, we deduce Equation
116 7 by integrating Equation 6:

$$C_B(t) = C_M \frac{k_1}{k_2}\left(1 - e^{-k_2 t}\right) \quad \text{Equation 7}$$

where k_1 is the uptake rate of metal in the biofilm (d^{-1}), and k_2 is the elimination rate constant (d^{-1}). Equation 7 corresponds to a two-compartment kinetic model (Landrum *et al.* 1992) where k_1 is considered as a constant under the assumption that the free binding sites concentration is in large excess compared to C_M. Former studies used this type of model to describe the accumulation of metal in biofilm (Bradac *et al*. 2009, Hill and Larsen 2005). $C_B(t)$ is rigorously the metal concentration in the biofilm at a given time t. Here the mean metal concentration in the biofilm between 0 and t ($\overline{C_B}$ in Equation 5) is approximated to $C_B(t)$ for every t.

Combining Equation 5 and Equation 7 gives the following Equation 8:

$$J = J_0 - C_M \frac{D_{MDL}}{\Delta_{MDL}} \frac{k_1}{k_2}\left(1 - e^{-k_2 t}\right) \quad \text{Equation 8}$$

$$\mathbf{J = J_0 - \alpha\left(1 - e^{-\beta t}\right)} \quad \text{Equation 9}$$

Where $\alpha = C_M \frac{D_{MDL}}{\Delta_{MDL}} \frac{k_1}{k_2}$ and $\beta = k_2$ Equation 10

3. Experimental section

3.1 DGT deployment in the Seine River

Twenty-four DGTs equipped with restricted gels (acrylamide with 0.8% bis-acrylamide cross-linker) and protective membranes: polyethersulfone-PES (0.45 µm pore diameter, 2.5 cm diameter, 140 µm thickness, Pall, Port Washington, New York, USA), and twenty-four DGTs equipped with restricted gels, protective membranes PES and Polycarbonate nuclepore membranes PC (0.4 µm pore diameter, 2.5 cm diameter, 10 µm thickness, Whatman, Little Chalfont, UK) were deployed in the Seine River, 40 km upstream of Paris, from 27th March 2012 to 18th April 2012. Accumulation of metals in Chelex resin was followed for 22 days by retrieving 6 DGTs of each type (PES and PC) at t=3, 8, 15, and 22 days (Figure 2). New triplicates of DGT of each type were deployed between: t=3 and t=8, t=8 and t=15, t=15 and t=22.

To measure total dissolved concentrations, two grab samples were collected with a plastic needle and filtered *in situ* (Minisart syringe filters with PES membranes, 0.45 µm, Sartorius, Göttingen, Germany) at time 3, 8, 15, and 22 days. Samples were acidified 1% vol. using suprapur HNO_3 (65% suprapur, Merck, Darmstadt, Germany) in the laboratory.

Moreover, grab samples were collected and filtered in situ to measure major ions (Ca^{2+}, Mg^{2+}, K^{+}, Na^{+}, NO_3^{-}, Cl^{-}, SO_4^{2-}, PO_4^{3-}, CO_3^{2-}) and also the dissolved organic carbon (DOC). pH, temperature were measured *in situ*. The data collected may be examined in the supporting information (Table SI 1).

3.2 DGT treatment

DGTs retrieved at time 3, 8, 15, and 22 days were dismantled and metals were eluted from the Chelex resin by soaking it in HNO_3 1 mol L^{-1}. PES and PC membranes were frozen (-80°C).

3.3 Total carbon measurements and scanning electron microscopy observations

To estimate the mass of deposits on membranes, the total carbon (TC) was analyzed using a LECO CS 125 analyser (St. Joseph, MI, USA) with a combustion of 900°C. Coupons (1 cm × 1 cm) were cut from protective membranes of DGT after exposure (at least three coupons for each immersion condition). Each coupon was immersed in 20 mL pure sterilized water and placed in an ultrasonic bath for 40 mins to remove the deposit. The sonication was stopped regularly and the water in the bath replaced with cold water to prevent the samples from overheating. Then the solution was filtered on a weighted and precombusted (4 hrs, 450°C) filter in fibreglass (GF/F, Whatman; diameter, 2 cm). The fibreglass filter was dried in a laboratory oven at 37°C overnight and then placed in a ceramic crucible directly in the furnace for combustion; accelerators (iron and tungsten) were required.

The biofilm attached to these membranes was observed by scanning electron microscopy (SEM). After exposure, the protective DGT membranes were rinsed in baths of pure water and then dehydrated under a formalin atmosphere in a fume hood; the surfaces were covered with a thin layer of gold/palladium prior to SEM imaging. All samples were imaged in an FEI Quanta 200 scanning electron microscope.

3.4 Metal analysis

Metals from DGTs and grab samples were analyzed using the ICP-MS (X series 2 Thermo Fisher Scientific, Villebon-sur-Yvette, France). Calibration of the ICP-MS was verified by analysis of the certified reference material NIST 1640a (natural water): mean recovery = 98%.

3.5 Flux calculation

Equation 3 ($\mathbf{J = \frac{m}{tA}}$) was used to calculate the mean flux at time t, with m as the mass of metal accumulated on the resin at t and with A as the exposure area. The calculated flux J was plotted against t. The effective sampling area A_e taking into account lateral diffusion was used in the calculations. A_e was taken equal to 3.66 cm², according to Knutsson *et al.* (2014).

3.6 Labile concentration calculation

Previous studies showed that a diffusion boundary layer δ is created in front of the samplers when they are immersed in water (Garmo *et al.* 2006, Uher *et al.* 2013, Warnken *et al.* 2006). δ has to be taken into account in the calculations where possible. δ is considered as an additional diffusion layer where the diffusion coefficient of the free metal in water is D_W. Equation 4 becomes:

$$C_{DGT} = \frac{m}{tA_e}\left(\frac{\Delta_{MDL}}{D_{MDL}} + \frac{\delta}{D_W}\right) = J\left(\frac{\Delta_{MDL}}{D_{MDL}} + \frac{\delta}{D_W}\right) \quad \text{Equation 11}$$

When a linear relationship between the mass accumulated on the resin m and the time t exists, the slope of the linear model can be used to calculate a global labile concentration as follows:

$$C_{DGT} = \frac{slope}{A_e}\left(\frac{\Delta_{MDL}}{D_{MDL}} + \frac{\delta}{D_W}\right) \quad \text{Equation 12}$$

The diffusion coefficients D_{MDL} used in this study were calculated in a previous study where we showed that protective membranes had no influence on the overall diffusion coefficient of the diffusion layer with restricted gels (Uher *et al.* 2012). D_W were taken from Li *et al.* (1974). D_{MDL} and D_W were corrected for the *in situ* temperature according to Zhang and Davison (1995).

The flow rate in the Seine River was high (109 ± 10 m^3 s^{-1}). No significant precipitations occurred and the flow rate remained fairly stable during the deployment, so the diffusive boundary layer thickness δ was taken to be constant over the deployment. As we dealt with fast-flowing water δ was set at 0.026 cm, as calculated in our previous study (Uher *et al.* 2013).

3.7 Model fitting

Fluxes J according to the time were calculated for DGTs deployed at d = 0. The models described in the theoretical background were fitted to the experimental data using nonlinear regression of the XLStat © software. J_0, α and β are the regression coefficients of the nonlinear model. Limits of the model were calculated with the limit values of the 95% confidence intervals of the parameters: upper limit = J calculated with J_{0max}, α_{min}, β_{min}, lower limit = J calculated with J_{0min}, α_{max}, β_{max}.

4. Results and discussion

4.1 Dissolved metal concentration

Total dissolved concentrations in Cr, Co, Cu, Mn, Ni, Pb, and Zn measured from day 0 (first day of the deployment) to day 22 are represented in Figure SI 1. Total dissolved concentrations were fairly stable over time, except for Cu, which increased at time t = 3 and t = 5 days, and for Zn. A discrepancy between the replicates was also observed: 40% for Cr at d3 and d15, 30% for Mn at d22.

4.2 Biofilm growth at the surface of the membranes

The total carbon measured on the membranes' surface over time is represented in Figure 3. The mass of carbon clearly increased with time, indicating that the biofilm grew steadily during the deployment. This result is supported by the SEM images (Figure 4) showing the biomass growing with time. At time t = 22 days, the membranes were colonized by diatoms. These results are consistent with those shown by Feng *et al.* (2016), who observed that the biofouling area was dominated by diatoms after 15 days deployment.

Figure 3 also shows that the biofilm growth was considerably higher on PES membranes from time t = 15 days. This is explained by the presence of a larger number of diatoms, as seen in Figure 4. Standard deviations were high, showing that biofilm colonization was heterogeneous depending on the samples.

4.3 Metal accumulation in the DGT

The amount of metals accumulated on the resin of the DGTs was monitored throughout the deployment. The metal accumulation patterns are shown in Figure SI-2 in the supporting information. Despite the higher biofilm growth on

PES membranes, no significant difference was observed between those DGTs equipped with both PES and PC membranes and DGTs equipped with PES membranes. Only the Pb accumulation pattern suggests a trend towards greater accumulation when DGTs were covered with PES membrane only (not statistically significant). Diatoms, which were more present on PES membranes, are phototrophic organisms that may lead to elevated pH inside the photosyntetically active biofilms (Liehr *et al.* 1994, Roeselers *et al.* 2008). This may favor removal of metals by precipitation. Here the metal accumulation by DGTs was not influenced by the phototrophic nature of the biofilms, except for Pb for which accumulation might be enhanced when diatoms are present.

Cd, Co, Cu, Mn, and Ni accumulations show a globally increasing trend between time t = 0 and time t = 22 (Spearman's correlation tests between m and t: p-values were respectively 5.10^{-6}, 3.10^{-8}, 7.10^{-11}, 3.10^{-8}, 7.10^{-15}). However, accumulation of Cr and Pb was less clear: the signal seems to remain stable because of the great variability of the experimental points, even if they are all above the limit of detection LD (LD = average value of the blanks + 3 × standard deviation on the blanks, n=8). Zn accumulation increased between day 0 and day 3, then seemed to increase from day 8 but the difference between day 8 and day 22 was not significant (Wilcoxon test, p = 0.09).

Replicates exhibited great variability (around 300%). Several sources of uncertainty were highlighted by Knutsson *et al*. (2014) such as preparation, handling of the samplers, and the diffusional pathway. Here, after a long deployment time (22 days), the variability of the replicates remained unchanged. After such a long period of time, the influence of blanks decreased significantly because of greater mass accumulation of metals. We thus assume that *in situ* conditions may play a role in the variability of the replicates, such as, for instance the position in the water column. We also noted that biomass greatly varied from one sample to another (Figure 3). Heterogeneous biofilm colonization may also explain the variability of the replicates.

The accumulation kinetics of DGTs deployed at time t = 0 were compared to accumulation kinetics built from the renewed DGTs, computed as follows: to calculate the average mass of metal at time t = 8 days, the average mass of metal accumulated by DGTs between time t = 3 and time t = 8 days was added to the average mass of metal accumulated at time t = 3, and so on until time t = 22 days. Because no significant difference was observed between DGTs equipped with both PES and PC membranes and DGTs equipped with PES membranes only, accumulation kinetics were represented by the mean of all DGT replicates. Examples of Co, Cu, and Zn are presented in Figure 5

while other metals are presented in the supporting information (see Figure SI-3). The kinetics built from renewed DGTs clearly increased more linearly than the kinetics from DGTs deployed at time t = 0 and are significantly higher. A plateau was reached for all metals except Ni for DGTs deployed at time t = 0. There was a substantial difference between the cumulated mass of renewed DGTs and the DGTs deployed for 22 days at the end of the deployment (on average 67%).

Deployment conditions clearly affected the DGT measurement. We will now try to discuss what factors led to this difference between renewed and initial DGTs.

Two studies in the recent literature provide useful indications. Firstly, Mongin *et al.* (2013) studied the limits of the linear accumulation regime of DGTs and concluded that a low pH (<5), a high metal concentration, a long time, or a high concentration of ligands can affect the linear regime of the DGTs. In the experiment reported in this article, pH was around 8.46 and in favor of a linear regime. The metal concentrations in the Seine River were lower than 5.10^{-8} mol L^{-1} for each metal while concentrations leading to a divergence of the linear regime in the study reported by Mongin *et al*. (2013) were in the order of 10^{-3} mol L^{-1}. Not more than 8 days were tested in the study of Mongin *et al*. (2013), so we are unable to draw conclusions on the time deployment. That being said if time affects the DGT measurement the pH conditions in the Seine River would argue more in favour of a linear regime.

Secondly, one significant characteristic of the Seine River is the calcium concentration (around 117 mg L^{-1} ≈ 2.9 mmol L^{-1}). Tankéré-Muller *et al.* (2012) studied the effect of the competitive cation binding of metals by DGT in marine waters. They concluded that measurement of Mn, which has a weak affinity for Chelex 100 resin, was strongly affected by the competition with Ca^{2+} at 10 mmol L^{-1} (approximately a 25% decrease). However, Co, which was included as a control metal having a higher affinity for Chelex 100 than Mn, was much less affected (with a deviation less than 10%). In our study deviations exist for all metals including those having the best affinity for the resin (Cu, Pb, Co) and are above 25%. If the presence of relatively high concentrations of Ca^{2+} affect the DGT measurement, especially for Mn, this does not fully explain the difference we observed in the Seine River. As well as these parameters we suggest that biofouling may play a role in the decrease of the DGT measurement with respect to time.

4.5 Flux in the DGTs and biofilm effect

The plot of flux in the DGTs with time shows that flux decreases for all metals (Figure 6 and Figure SI 4). If we suppose that metal concentrations in water are relatively constant (except for Cu), the flux should be constant. Here we observe a sharp decrease during the first days of deployment, followed by a plateau at the end (Co, Zn), probably related to the plateaus observed for the metal accumulation in DGTs deployed at time t = 0 (Figure 5). To verify the hypothesis that biofouling can affect the DGT measurement, we tried to fit the experimental data with the models described in the theoretical background. As no significant difference was observed between DGTs equipped with PES and PC membranes and DGTs equipped with PES membranes only, all the DGT replicates deployed at t = 0 were used to fit the model in order to improve the statistical power of the model.

The interaction model described by Equation 8 fits the data of DGTs deployed at t = 0 for Co and Zn very well with, respectively, R^2=0.78 and 0.79 (Figure 6). The same pattern was observed for Cd, Mn, and Ni (R^2=0.41, 0.51, 0.79; see SI). When fluxes of DGTs deployed later (at time t = 3, 8, and 15 days) are added to the graphs according to the deployment time, they fit the model for Co and Zn. However, they fit the model in a lesser extent for Cd, Mn and Ni although replicates exhibit a great variability for these metals. This is in agreement with the hypothesis that concentrations were relatively constant for these metals during deployment. For them the fluxes depend more on the number of days DGTs were deployed rather than the moment where they were deployed. Regarding Cu, the flux seems to decrease linearly with time and does not follow the nonlinear Equation 8. However, as we know, the Cu concentrations were not constant during the deployment and thus did not meet one of the assumptions of the model of Equation 8. We cannot therefore conclude about Cu.

Moreover, Cr and Pb (see Figure SI 4) do not follow the model either. This could be related to the fact that accumulation of Cr was not significant enough for these elements (see Figure SI 2 and the section on metal accumulation), or else to the great variability of Pb replicates. Furthermore, other processes not taken into account in the model may occur.

In conclusion, the decrease of the metal flux in DGTs during deployment seems to be correctly defined by the metal–biofilm interaction model for Cd, Co, Mn, Ni, and Zn. This model gives a suitable explanation as to why the biofouling effect on the measurement may depend on the metal and highlights the kinetic aspect of the biofouling

effect. However, other processes may occur. For instance we choose to neglect MDL increase in our model. Models involving MDL increase tested with our data (data not shown) were unsuccessful. A model combining both MDL increase and metal-biofilm interactions would be an issue, but requires more data than we had to correctly fit such a model.

4.6 Kinetic constants and labile concentrations

For Cd, Co, Mn, Ni, and Zn, the parameters of the regression J_0, α and β were estimated. From the latter, uptake and elimination rate constants k_1 and k_2 were calculated in s^{-1} and d^{-1} using Equation 10 and may be seen in Table 1, except k_1 for Cd for which C_W was under the limit of quantification. The characteristic time $t_{1/2}$ corresponding to the time where the flux is equal to 50% of the initial flux was also calculated with

$$t_{1/2} = -\frac{1}{\beta}\ln\left(1 - \frac{J_0}{2\alpha}\right) \qquad \text{Equation 13}$$

The initial labile concentration, which was not affected by biofouling, was calculated from J_0 following Equation 11:

$$C_0 = J_0\left(\frac{\Delta g}{D} + \frac{DBL}{D_w}\right) \qquad \text{Equation 14}$$

C_0 was compared with the mean dissolved concentration measured in water C_W by calculating the C_0/C_W ratio. C_0 was consistent for Cd and was lower than the Cd labile concentrations found by Tusseau-Vuillemin *et al.* (2007) in the Seine River. For Co and Ni, C_0 was lower than C_W, as can be expected from a labile concentration, and in the range of values found by Tusseau-Vuillemin *et al*. The C_0/C_W ratio was also the same as in the Tusseau-Vuillemin *et al*. study for Ni, but larger for Co. In the case of Mn and Zn, C_0 was overestimated but was on the same order of magnitude as C_W.

k_2 was in the same order of magnitude as k_1. It illustrates that the biosorption mechanism is based on a number of metal-binding processes taking place with components of the biofilm components' cell wall. The cell walls can reversibly biosorb metals and thus function in a similar way to an ion-exchange resin (Wase and Wase 2002). k_2 represents the dissociation of the metal from the biofilm, which is driven by the DGT gradient strength and must be higher to allow the accumulation of metal by Chelex resin (Co and Ni). The values of k_1 calculated here are in the same order of magnitude as the water rate constant of Cr^{3+} ($k_w=5.10^{-7}$ s^{-1}), which is considered to be very slow in comparison to the water rate constants of other metals ($k_w(Cd^{2+})=3.10^8$ s^{-1}, $k_w(Co^{2+})=2.10^6$ s^{-1}) (Stumm and Morgan

1996). The association of metals with the biofilm grown at the surface of DGTs is therefore a slow reaction because of the predominant DGT gradient strength. However, some of the metal might be trapped. This is highlighted by the calculation of the characteristic time $t_{1/2}$, presented in Table 1, which shows that the flux is very quickly affected during the deployment and decreases within the first few days: in the case of Co, the flux was decreased by 50% in just 4 days.

To obtain the $C_{DGT\text{-}m}$, that is, the mean labile concentration of the metals in the Seine River that were the least affected by *in situ* and physicochemical conditions, C_{DGT} was derived from the slope of the accumulation kinetics of the renewed DGTs (See Figure 5) using Equation 12 (Tusseau-Vuillemin *et al*. 2007). The resulting labile concentrations are given in Table 2. The labile concentration $C_{DGT\text{-}T22}$ calculated from the mass accumulated in DGTs at time t = 22 days using Equation 11 are also presented.

Labile concentrations from the renewed DGTs were in the same order of magnitude as the concentrations measured in the Seine River basin reported by Tusseau-Vuillemin *et al*. (2007) in which the deployment took 8 days. Labile percentages ranged from 21 to 202%. It would be interesting to investigate Mn, Pb, and Zn in order to determine if the high value of $C_{DGT\text{-}m}$ stems from possible contamination peaks that eluded the grab samples or raises questions regarding the technique and the calculations themselves.

The $C_{DGT\text{-}T22}$ was underestimated two- to sevenfold when compared with $C_{DGT\text{-}m}$. This highlights the difference between that of a long deployment time affected as it is by environmental and physicochemical conditions and that of a shorter deployment time.

5. Conclusion

The quantitative model that has been proposed to highlight the biofouling effect was able to explain the decrease observed on the flux toward the DGT resin of Cd, Co, Mn, Ni, and Zn on the presented data. Although other processes not examined in this model may occur, the hypothesis that metals would be temporarily retained by the biofilm at the surface of the DGTs because of interactions within the biofilm is credible in the conditions of our study. In the conditions we studied we would recommend a deployment time of 5 to 8 days to minimize the biofouling effect. However, biofouling is inevitable. The biofouling effect should certainly be considered as being a part of the *in situ* DGT response. Therefore *in situ* speciation results should be considered with care.

However these kinetic processes may be dependent on the metal and the sampling site. Some strong effects observed in our study may not happen in different conditions. More data in different conditions are needed to document biofouling effect.

ASSOCIATED CONTENT

Supporting Information. Physicochemical parameters of the Seine River, the total dissolved concentration of metal in water and metal accumulation patterns in the DGTs during the deployment, accumulation kinetics in the DGTs, and the metal flux in the DGTs during the deployment are available as supporting information.

AUTHOR INFORMATION

Corresponding Author

* E-mail: emmanuelle.uher@irstea.fr; Tel: +33 1 40 96 65 39; Fax: +33 1 40 96 61 99.

Funding Sources

This study is part of the EMESTox project, funded by the French National Research Agency.

Acknowledgments

Sophie Ayrault (Laboratoire des Sciences du Climat et de l'Environnement, Gif-sur-Yvette, France) is acknowledged for providing access to ICP–MS, as is Nicolas Gayet (Laboratoire Environnement Profond, Ifremer, Brest) for his helpful technical support and expertise in total carbon measurements and SEM observations.

References

Booij K, van Bommel R, Mets A, Dekker R (2006): Little effect of excessive biofouling on the uptake of organic contaminants by semipermeable membrane devices. Chemosphere 65, 2485-2492

Bradac P, Behra R, Sigg L (2009a): Accumulation of Cadmium in Periphyton under Various Freshwater Speciation Conditions. Environ. Sci. Technol. 43, 7291-7296

Bradac P, Navarro E, Odzak N, Behra R, Sigg L (2009b): Kinetics of cadmium accumulation in periphyton under freshwater conditions. Environ. Toxicol. Chem. 28, 2108-2116

359 Bradac P, Wagner B, Kistler D, Traber J, Behra R, Sigg L (2010): Cadmium speciation and accumulation in
360 periphyton in a small stream with dynamic concentration variations. Environ. Pollut. 158, 641-648

361 Buzier R, Charriau A, Corona D, Lenain JF, Fondaneche P, Joussein E, Poulier G, Lissalde S, Mazzella N, Guibaud
362 G (2014): DGT-labile As, Cd, Cu and Ni monitoring in freshwater: Toward a framework for interpretation of in situ
363 deployment. Environ. Pollut. 192, 52-58

364 Davison W, Zhang H (2012): Progress in understanding the use of diffusive gradients in thin films (DGT) - back to
365 basics. Environ. Chem. 9, 1-13

366 Duong TT, Morin S, Coste M, Herlory O, Feurtet-Mazel A, Boudou A (2010): Experimental toxicity and
367 bioaccumulation of cadmium in freshwater periphytic diatoms in relation with biofilm maturity. Sci. Total Environ.
368 408, 552-562

369 Faburé J, Dufour M, Autret A, Uher E, Fechner LC (2015): Impact of an urban multi-metal contamination gradient:
370 Metal bioaccumulation and tolerance of river biofilms collected in different seasons. Aquat. Toxicol. 159, 276-289

371 Fechner LC, Gourlay-Francé C, Tusseau-Vuillemin MH (2014): Linking community tolerance and structure with
372 low metallic contamination: A field study on 13 biofilms sampled across the seine river basin. Water Res. 51, 152-
373 162

374 Feng ZM, Zhu P, Fan HT, Piao SS, Xu L, Sun T (2016): Effect of Biofilm on Passive Sampling of Dissolved
375 Orthophosphate Using the Diffusive Gradients in Thin Films Technique. Anal. Chem. 88, 6836-6843

376 Garmo OA, Naqvi KR, Royset O, Steinnes E (2006): Estimation of diffusive boundary layer thickness in studies
377 involving diffusive gradients in thin films (DGT). Anal. Bioanal. Chem. 386, 2233-2237

378 Garmo OA, Davison W, Zhang H (2008a): Effects of Binding of Metals to the Hydrogel and Filter Membrane on the
379 Accuracy of the Diffusive Gradients in Thin Films Technique. Anal. Chem. 80, 9220-9225

380 Garmo OA, Davison W, Zhang H (2008b): Interactions of trace metals with hydrogels and filter membranes used in
381 DET and DGT techniques. Environ. Sci. Technol. 42, 5682-5687

382 Ginisty P, Besnainou B, Sahut C, Guezennec J (1998): Biosorption of cobalt by Pseudomonas halodentrificans:
383 influence of cell wall treatment by alkali and alkaline-earth metals and ion-exchange mechanisms. Biotechnol. Lett.
384 20, 1035-1039

385 Hill WR, Larsen IL (2005): Growth dilution of metals in microalgal biofilms. Environ. Sci. Technol. 39, 1513-1518

386 Knutsson J, Rauch S, Morrison GM (2014): Estimation of Measurement Uncertainties for the DGT Passive Sampler
387 Used for Determination of Copper in Water. Int. J. Anal. Chem.

388 Kuyucak N, Volesky B (1988): Biosorbents for recovery of metals from industrial solutions. Biotechnology Letters
389 10, 137-142

390 Landrum PF, Lee H, Lydy MJ (1992): Toxicokinetics in aquatic systems - model comparisons and use in hazard
391 assessment. Environ. Toxicol. Chem. 11, 1709-1725

392 Li W-W, Yu H-Q (2014): Insight into the roles of microbial extracellular polymer substances in metal biosorption.
393 Bioresour. Technol. 160, 15-23

394 Li Y, Gregory, S. (1974): Diffusion of ions in sea water and in deep-sea sediments. Geochim. Cosmochim. Acta 38,
395 703-714

396 Liehr SK, Chen H-J, Lin S-H (1994): Metals removal by algal biofilms. Water Sci. Technol. 30, 59-68

397 Mongin S, Uribe R, Rey-Castro C, Cecilia J, Galceran J, Puy J (2013): Limits of the Linear Accumulation Regime
398 of DGT Sensors. Environ. Sci. Technol. 47, 10438-10445

399 Moppert X, Le Costaouec T, Raguenes G, Courtois A, Simon-Colin C, Crassous P, Costa B, Guezennec J (2009):
400 Investigations into the uptake of copper, iron and selenium by a highly sulphated bacterial exopolysaccharide
401 isolated from microbial mats. J. Ind. Microbiol. Biotechnol. 36, 599-604

402 More TT, Yadav JSS, Yan S, Tyagi RD, Surampalli RY (2014): Extracellular polymeric substances of bacteria and
403 their potential environmental applications. J. Environ. Manage. 144, 1-25

404 Nimick DA, Gammons CH, Parker SR (2011): Diel biogeochemical processes and their effect on the aqueous
405 chemistry of streams: A review. Chem. Geol. 283, 3-17

406 Pichette C, Zhang H, Davison W, Sauve S (2007): Preventing biofilm development on DGT devices using metals
407 and antibiotics. Talanta 72, 716-722

408 Roeselers G, Loosdrecht MCMv, Muyzer G (2008): Phototrophic biofilms and their potential applications. J. Appl.
409 Phycol. 20, 227-235

410 Schafer RB, Paschke A, Liess M (2008): Aquatic passive sampling of a short-term thiacloprid pulse with the
411 Chemcatcher: Impact of biofouling and use of a diffusion-limiting membrane on the sampling rate. J. Chromatogr. A
412 1203, 1-6

413 Stumm W, Morgan J (1996): Aquatic geochemistry. Chemical Equilibria and Rates in Natural Waters, A Wiley-
414 Interscience Publication, New York

415 Tankere-Muller S, Davison W, Zhang H (2012): Effect of competitive cation binding on the measurement of Mn in
416 marine waters and sediments by diffusive gradients in thin films. Anal. Chim. Acta 716, 138-144

417 Toner B, Manceau A, Marcus MA, Millet DB, Sposito G (2005): Zinc sorption by a bacterial biofilm. Environ. Sci.
418 Technol. 39, 8288-8294

419 Tusseau-Vuillemin MH, Gourlay C, Lorgeoux C, Mouchel JM, Buzier R, Gilbin R, Seidel JL, Elbaz-Poulichet F
420 (2007): Dissolved and bioavailable contaminants in the Seine river basin. Sci. Total Environ. 375, 244-256

421 Uher E, Zhang H, Santos S, Tusseau-Vuillemin M-H, Gourlay-Francé C (2012): Impact of Biofouling on Diffusive
422 Gradient in Thin Film Measurements in Water. Anal. Chem. 84, 3111-3118

423 Uher E, Tusseau-Vuillemin MH, Gourlay-Francé C (2013): DGT measurement in low flow conditions: diffusive
424 boundary layer and lability considerations. Env. Sci. Process. Impact 15, 1351-1358

425 Van Hullebusch ED, Zandvoort MH, Lens PN (2003): Metal immobilisation by biofilms: Mechanisms and
426 analytical tools. Rev. Environ. Sci. Bio/Technol. 2, 9-33

427 Veglio F, Beolchini F (1997): Removal of metals by biosorption: A review. Hydrometallurgy 44, 301-316

428 Warnken KW, Zhang H, Davison W (2006): Accuracy of the diffusive gradients in thin-films technique: Diffusive
429 boundary layer and effective sampling area considerations. Anal. Chem. 78, 3780-3787

430 Wase DAJ, Wase J (2002): Biosorbents for Metal Ions. CRC Press

431 White C, Gadd GM (2000): Copper accumulation by sulfate-reducing bacterial biofilms. FEMS Microbiol. Lett.
432 183, 313-318

433 Zhang H, Davison W (1995): Performance-Characteristics of Diffusion Gradients in Thin-Films for the in-Situ
434 Measurement of Trace-Metals in Aqueous-Solution. Anal. Chem. 67, 3391-3400

435

436

437

In situ measurement with diffusive gradients in thin films: effect of biofouling in freshwater

Emmanuelle Uher[*1,2], Chantal Compère[3], Matthieu Combe[1], Florence Mazeas[3], Catherine Gourlay-Francé †[1,2].*

Figures and tables

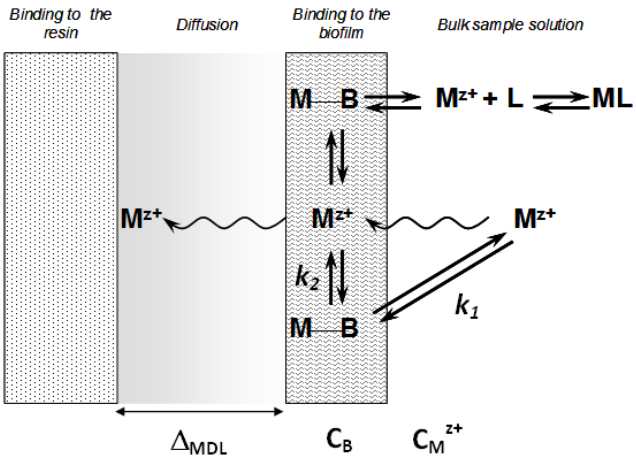

Figure 1- Schematic representation of the role of the biofilm in the accumulation of metal by DGT (adapted from Uher et al. 2011)

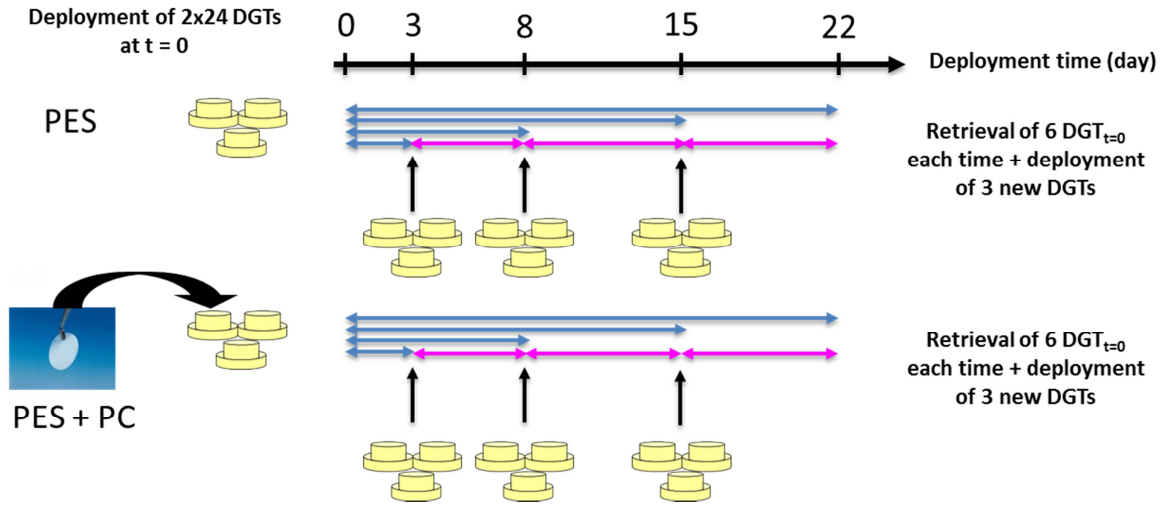

Figure 2 – Deployment scheme of the DGTs in the Seine River

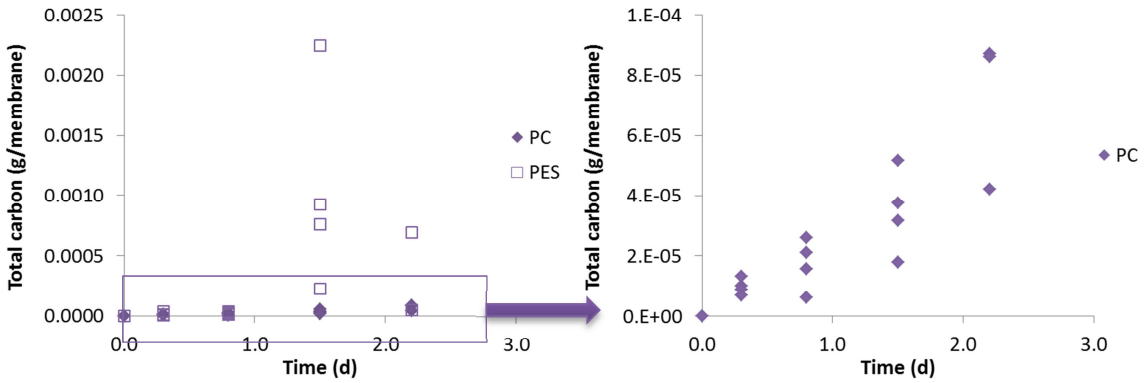

Figure 3 – Total carbon per membrane over time

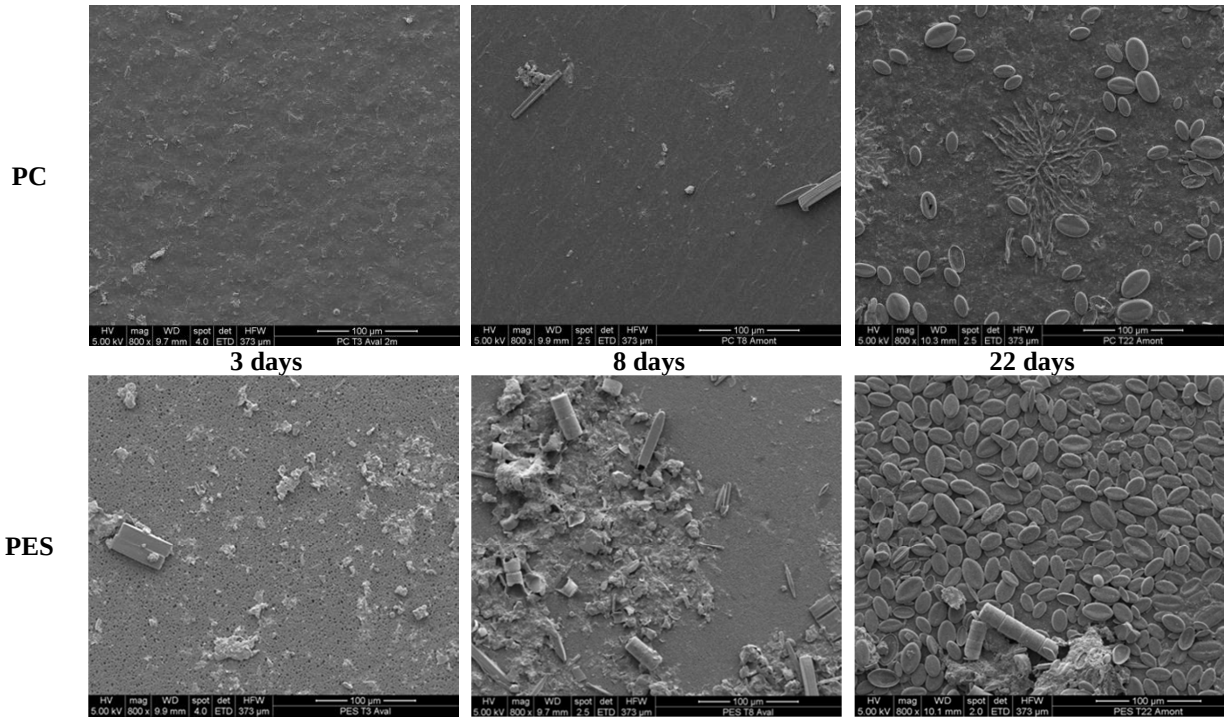

Figure 4 – SEM pictures of the biofilm attached to the membranes over time

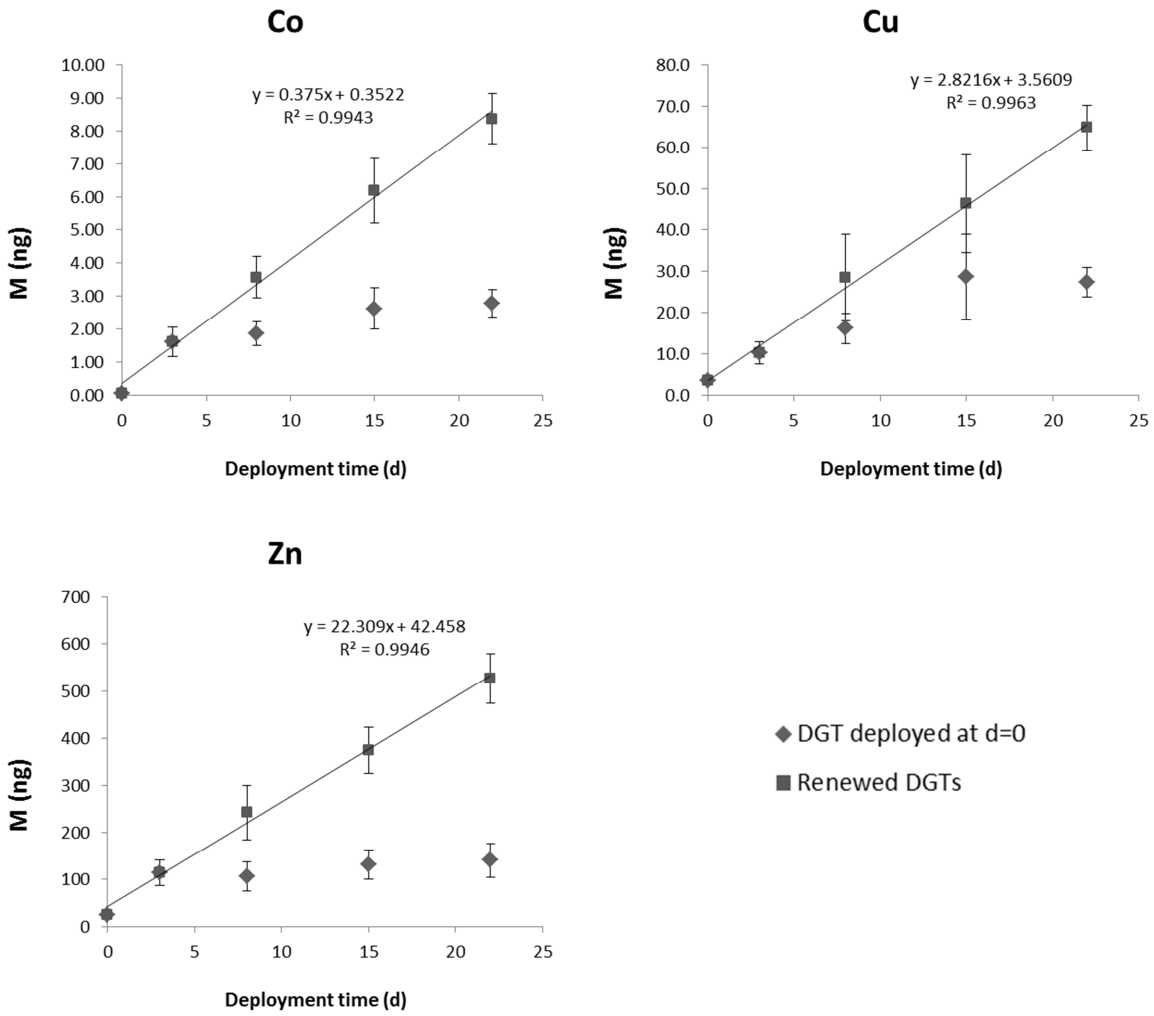

Figure 5 – Accumulation kinetics in all the DGTs deployed at t=0 and in all the renewed DGTs. Bars represent standard deviations.

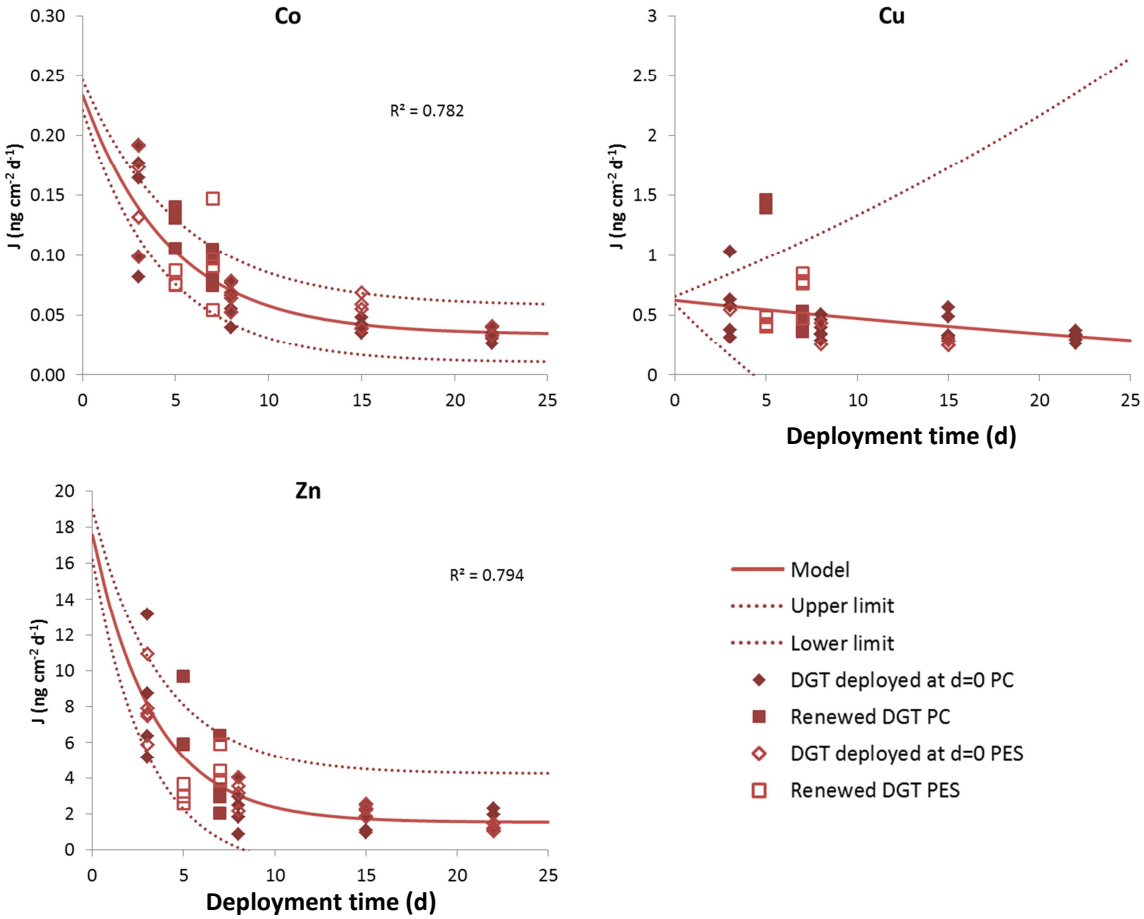

Figure 6 - Metal flux in the DGTs during the deployment and model fitting the data of DGTs deployed at d = 0 and including PES and PC. DGTs deployed at t=0 are represented by diamonds. Open symbols represent DGTs equipped with PES membranes, and filled symbols represent DGTs equipped with PC membranes. Upper and lower limits were calculated with the minima and maxima values of the parameters confidence intervals.

	Cd	Co	Mn	Ni	Zn
J_0 (ng cm^{-2} s^{-1})	$1.10x10^{-7}$	$2.67x10^{-6}$	$1.70x10^{-4}$	$2.27x10^{-5}$	$2.00x10^{-4}$
C_0 (µg L^{-1}) (% C_0/C_W)	0.0045 n.c	0.11 (60%)	6.8 (319%)	0.93 (46%)	6.8 (308%)
k_1 (s^{-1}) (d^{-1})	n.c n.c	$1.11x10^{-6}$ 0.096	$4.06x10^{-6}$ 0.35	$7.92x10^{-7}$ 0.068	$8.29x10^{-6}$ 0.72
k_2 (s^{-1}) (d^{-1})	$1.33x10^{-6}$ 0.11	$2.45x10^{-6}$ 0.21	$1.84x10^{-6}$ 0.16	$2.46x10^{-6}$ 0.21	$3.43x10^{-6}$ 0.30
$t_{1/2}$ (d)	9.0	4.1	6.4	4.5	2.7

Table 1. Initial flux, initial labile concentration, uptake, and elimination rate of the metal in the biofilm and half-time of the flux calculated from the parameters of the nonlinear regression.

	Cd	Cr	Co	Cu	Mn	Ni	Pb	Zn
C_{DGT-m} (µg L^{-1}) (% C_{DGT}/C_W)	0.0049 n.c	0.21 (33%)	0.048 (27%)	0.34 (29%)	4.3 (202%)	0.44 (21%)	0.25 (183%)	2.4 (108%)
$C_{DGT-T22}$ (µg L^{-1}) (% C_{DGT}/C_W)	0.0020 n.c	0.058 (9%)	0.016 (9%)	0.15 (13%)	1.6 (74%)	0.19 (10%)	0.034 (25%)	0.68 (31%)

Table 2. Labile concentration calculated from accumulation kinetics of the renewed DGTs and labile concentrations calculated from mass accumulated at t=22 days. Labile percentage in relation to the dissolved concentration in parentheses

SUPPORTING INFORMATION

	pH	T°	Ca^{2+}	K^{+}	Mg^{2+}	Na^{+}	Cl^{-}	NO_3^{-}	PO_4^{3-}	SO_4^{2-}	CO_3^{2-}	DOC
Units	-	°C	mg L^{-1}	mg L^{-1}	mg L^{-1}	mg L^{-1}	mg L^{-1}	mg L^{-1}	mg L^{-1}	mg L^{-1}	mg L^{-1}	mg L^{-1}
Mean	8.46	13.09	117.0	2.356	2.33	10.5	19.1	21.85	n.d	22.48	266	2.48
CI 95%	0.13	0.79	9.2	0.087	0.17	1.7	2.8	0.51	n.d	0.92	20	0.31

Table SI 1 – Physicochemical parameters of the Seine River during the deployment. Concentrations are the mean of 6 (Ca^{2+}, K^{+}, Mg^{2+}, Na^{+}, Cl^{-}, NO_3^{-}, SO_4^{2-}), 8 (T°) and 9 (CO_3^{2-}, DOC, pH) grab samples. n.d = not detected. CI : confidence interval 95%

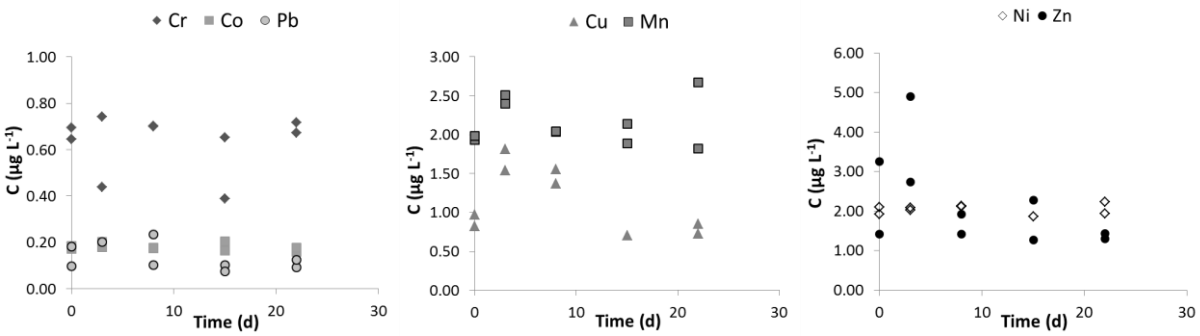

Figure SI 1 - Total dissolved concentration in µg L^{-1} during the deployment

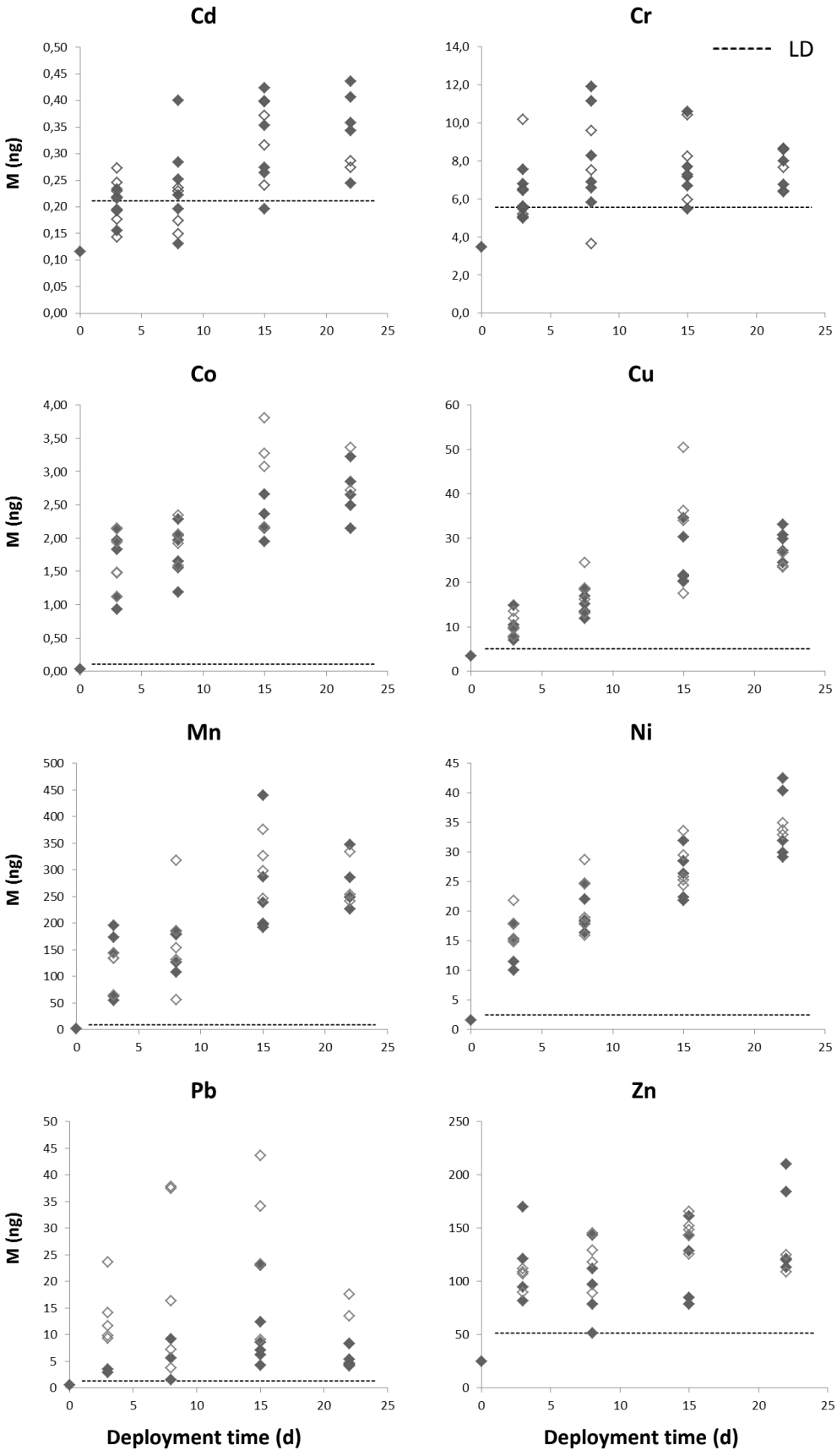

Figure SI 2 – Metal accumulation patterns in the DGTs during the deployment. Open symbols: DGTs equipped with PES membranes. Closed symbols: DGTs equipped with PES+PC membranes

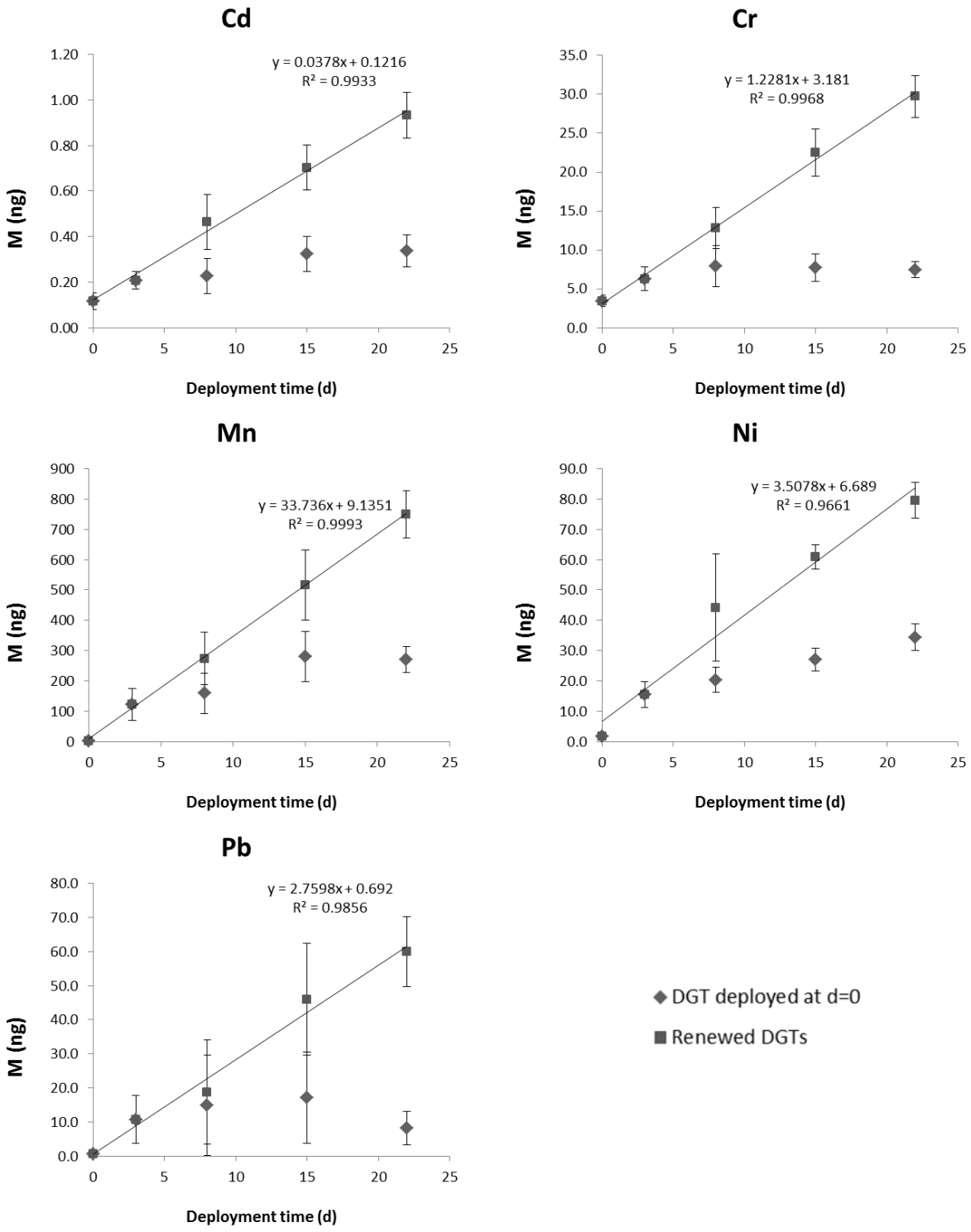

Figure SI 3 – Accumulation kinetics in all the DGTs deployed at d = 0 and in all the renewed DGTs. Bars represent standard deviations.

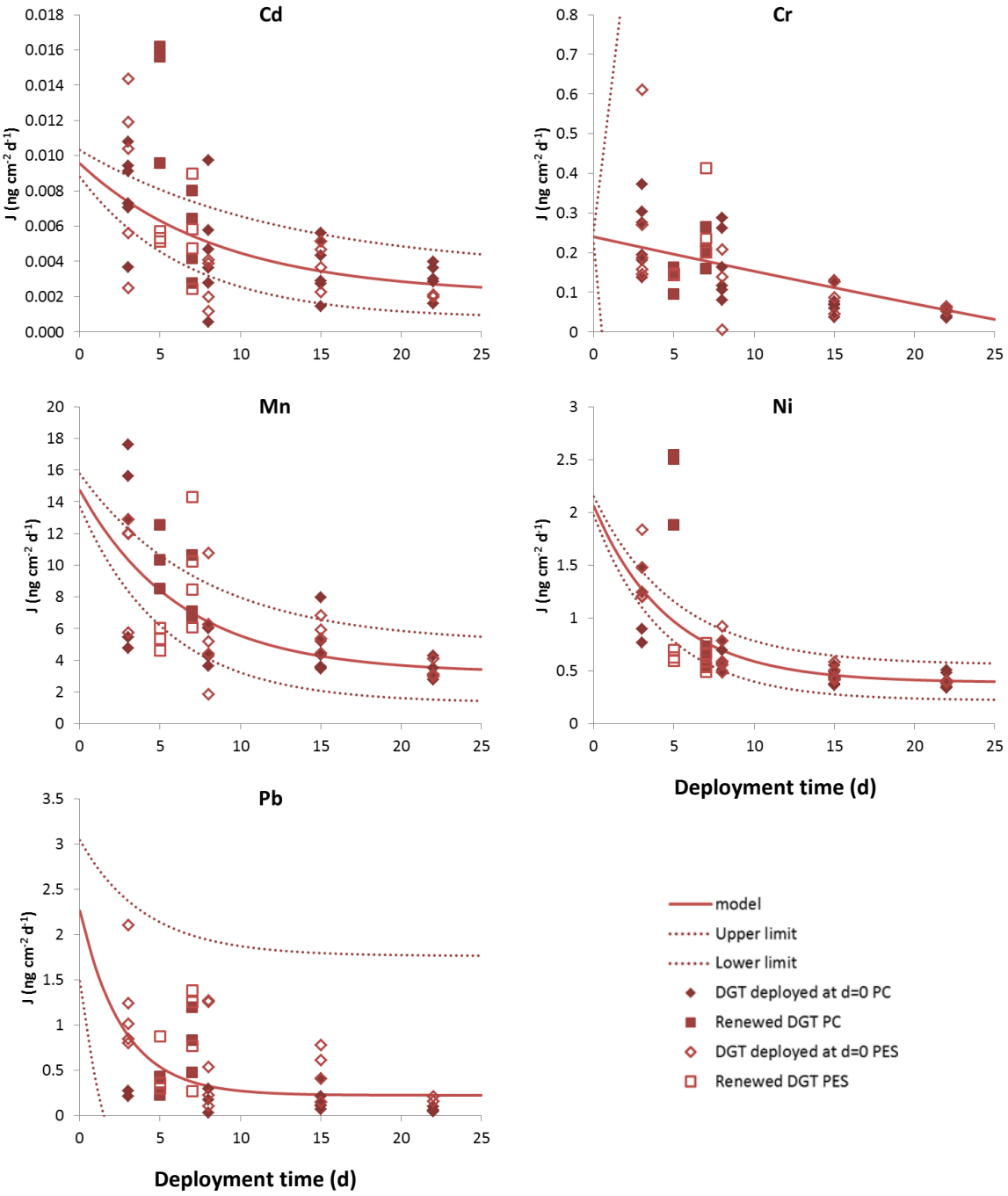

Figure SI 4 – Metal flux in the DGTs during the deployment and model fitting the data of DGTs deployed at d = 0 and including PES and PC. Upper and lower limits were calculated with the minima and maxima values of the parameters confidence intervals.